

sanctuary. Furthermore, therapeutic maneuvers designed to block the initial viremic phase of infection also may result in prevention of neurologic disease and could be tested in this model. We have shown that AZT dramatically alters the onset and course of retrovirus-induced neurologic disease in a dose-dependent manner. AZT effectively crosses the placental barrier and ameliorates disease in offspring infected in utero when treatment is given during gestation to the pregnant female. AZT therapy also leads to significant improvement in animals infected during the neonatal period. Thus, the murine neurotropic disease model permits rapid, cost-effective, quantitative assessments of treatment strategies that may be relevant to the therapy of neurologic manifestations of human retrovirus infections. Because AZT alters the onset and course of disease due to transplacental and perinatal retrovirus infection, we also can evaluate the efficacy of treatment during gestation and in the perinatal period, an important issue because of the increasing prevalence of pediatric AIDS (2).

- observations.
18. M. Gardner *et al.*, *J. Natl. Cancer Inst.* **58**, 1855 (1977); M. Gardner, J. Estes, J. Casagrande, S. Rasheed, *ibid.* **64**, 359 (1980).
  19. L. Des Grosseillers, M. Barrette, P. Jolicoeur, *J. Virol.* **52**, 356 (1986).
  20. We thank P. Jolicoeur for Cas-Br-E-producing cells; S. Nusinoff-Lehrman (Burroughs Wellcome, Inc.) for AZT; P. Chassler, R. Curry, D. Grottkopp, and L. O'Brien for their excellent technical assistance; and J. Andersen for help with statistical analy-

A.H.S. is a Lucille P. Markey Scholar and this work was supported in part by a grant from the Lucille P. Markey Charitable Trust. R.M.R. is the recipient of a faculty development award from the Pharmaceutical Manufacturers Association Foundation. Supported in part by a contract from Commonwealth of Massachusetts Department of Public Health and NIH grant U01-AI24845-01 to R.M.R. and by NIH grants HD19015 and CA38497 to R.J.

17 April 1987; accepted 2 June 1987

## Divalent Cations Directly Affect the Conductance of Excised Patches of Rod Photoreceptor Membrane

J. H. STERN, HANS KNUTSSON,\* P. R. MACLEISH

Phototransduction in rod cells is likely to involve an intracellular messenger system that links the absorption of light by rhodopsin to a change in membrane conductance. The direct effect of guanosine 3',5'-monophosphate (cGMP) on excised patches of rod outer segment membrane strongly supports a role for cGMP as an intracellular messenger in phototransduction. It is reported here that magnesium and calcium directly affect the conductance of excised patches of rod membrane in the absence of cGMP and that magnesium, applied to intact rod cells, blocks a component of the cellular light response. The divalent cation-suppressed conductance in excised patches showed outward rectification and cation-selective permeability resembling those of the light-suppressed conductance measured from the intact rod cell. The divalent cation-suppressed conductance was partly blocked by a concentration of the pharmacological agent *L-cis*-diltiazem that blocked all of the cGMP-activated conductance. Divalent cations may act, together with cGMP, as an intracellular messenger system that mediates the light response of the rod photoreceptor cell.

**F**ESENKO *et al.* (1) REPORTED THAT guanosine 3',5'-monophosphate (cGMP) directly activates the conductance of excised patches of rod cell membrane (1-5). We report here that, in the absence of cGMP, the divalent cations magnesium and calcium directly suppress the conductance of excised patches of rod membrane.

The effect of divalent cations on the rod membrane conductance was studied by exposing the intracellular side of inside-out, excised patches (6) to various bath concentrations of Ca<sup>2+</sup> and Mg<sup>2+</sup> (7). Patches were obtained from solitary rod photoreceptor cells dissociated from the tiger salamander retina (4, 8). In most experiments, the bath and pipette contained a simple salt solution of 120 mM NaCl, 3 mM KCl, 1 mM Hepes, and 0.02 mM phenol red at pH 7.3. In other experiments we used a stock solution containing 108 mM NaCl, 16 mM glucose, 3 mM KCl, 1 mM Hepes, 1 mM NaHCO<sub>3</sub>, 1 mM sodium pyruvate, 0.5 mM NaH<sub>2</sub>PO<sub>4</sub>, and 0.02 mM phenol red at pH 7.3. The pipette solution always contained an additional 1 or 2 mM CaCl<sub>2</sub> and 1 or 2 mM MgCl<sub>2</sub>, and the bath solution contained the Ca<sup>2+</sup> and Mg<sup>2+</sup> concentrations indicated. The bath solution was varied by moving the patch pipette to appropriate positions in

front of a linear array of superfusion pipettes (diameter, 100 μm). Suction pipettes were made with a BB-CH pipette puller and Drummond 100-μl microcaps or Corning type 7740 capillary tubing; those having a final tip diameter of 1 to 2 μm were used immediately from the puller.

A current-clamp experiment in which 15-pA current pulses were applied to an excised patch of rod outer segment membrane is shown in Fig. 1A. Initially, the intracellular side of the membrane was exposed to a solution lacking divalent cations (9) and the conductance was high, as indicated by the small voltage deflection. The bathing solution was then changed to one containing 1 mM Ca<sup>2+</sup>, and the conductance decreased two- to threefold. Changing the intracellular solution from 1 mM Ca<sup>2+</sup> to 1 mM Mg<sup>2+</sup> caused little further change (10). Figure 1A shows that both Ca<sup>2+</sup> and Mg<sup>2+</sup> caused rapid and reversible decreases in the patch membrane conductance in the absence of added cGMP. The effects of divalent cations were observed in this patch for 12 cycles of

### REFERENCES AND NOTES

1. B. A. Navia, B. D. Jordan, R. W. Price, *Ann. Neurol.* **19**, 517 (1986); B. A. Navia *et al.*, *ibid.*, p. 525; L. R. Sharer *et al.*, *Human Pathol.* **17**, 271 (1986); L. G. Epstein *et al.*, *Pediatrics* **78**, 678 (1986).
2. M. J. Cowan *et al.*, *Pediatrics* **73**, 382 (1984); N. Lapointe *et al.*, *N. Engl. J. Med.* **312**, 1325 (1985); E. Jovaisas *et al.*, *Lancet* **1985-II**, 1129 (1985); J. B. Ziegler *et al.*, *ibid.* **1985-I**, 896 (1985); G. B. Scott *et al.*, *J. Am. Med. Assoc.* **253**, 363 (1985); S. Pahwa *et al.*, *ibid.* **255**, 2299 (1986).
3. J. P. Horwitz, J. Chua, M. J. Noel, *J. Org. Chem.* **29**, 2076 (1964); T.-S. Lin, W. H. Prusoff, *J. Med. Chem.* **21**, 109 (1978); H. Mitsuya *et al.*, *Proc. Natl. Acad. Sci. U.S.A.* **82**, 7096 (1985); P. A. Furman *et al.*, *ibid.* **83**, 8333 (1986).
4. M. B. Gardner *et al.*, *J. Natl. Cancer Inst.* **51**, 1243 (1973); M. B. Gardner, *Curr. Top. Microbiol. Immunol.* **79**, 215 (1978); *Rev. Infect. Dis.* **7**, 99 (1985); P. Yuen *et al.*, *J. Virol.* **59**, 59 (1986).
5. C. K. Petito *et al.*, *N. Engl. J. Med.* **312**, 874 (1985); J. R. Swarz, B. R. Brooks, R. T. Johnson, *Neuropath. Appl. Neurobiol.* **7**, 365 (1981); B. R. Brooks, J. R. Swarz, R. T. Johnson, *Lab. Invest.* **43**, 480 (1980); M. B. A. Oldstone *et al.*, *Virology* **107**, 180 (1980); M. B. A. Oldstone *et al.*, *Am. J. Pathol.* **88**, 193 (1977).
6. N. Nathanson *et al.*, in *Viruses and Demyelinating Diseases*, L. Mims, M. Cuzner, L. Kelly, Eds. (Academic Press, New York, 1983), pp. 111-140.
7. R. Jaenisch, *Proc. Natl. Acad. Sci. U.S.A.* **73**, 1260 (1976); D. Jähner and R. Jaenisch, *Nature (London)* **287**, 456 (1980); R. Jaenisch *et al.*, *Cell* **24**, 519 (1981); C. Stewart, K. Harbers, D. Jähner, R. Jaenisch, *Science* **221**, 760 (1983); R. Jaenisch, *Virology* **93**, 80 (1979).
8. R. Jaenisch, *Cell* **19**, 181 (1980).
9. D. Jähner *et al.*, *Nature (London)* **298**, 623 (1982).
10. P. Nobis and R. Jaenisch, *Proc. Natl. Acad. Sci. U.S.A.* **77**, 3677 (1980).
11. J. Löhler and R. Jaenisch, unpublished observation.
12. A. H. Sharpe and R. Jaenisch, unpublished observations.
13. R. Yarchoan *et al.*, *Lancet* **1987-I**, 132 (1987); R. Yarchoan *et al.*, *ibid.* **1986-I**, 575 (1986).
14. H. Mitsuya and S. Broder, *Nature (London)* **325**, 773 (1987); R. Yarchoan and S. Broder, *N. Engl. J. Med.* **316**, 557 (1987).
15. R. M. Ruprecht, unpublished observations.
16. R. M. Ruprecht *et al.*, *Nature (London)* **323**, 467 (1986).
17. D. Trites, X.-M. Liu, R. Ruprecht, unpublished

Laboratory of Neurobiology, Rockefeller University, New York, NY 10021.

\*Permanent address: Department of Electrical Engineering, University of Linköping, Linköping, Sweden.

divalent cation application and removal. The divalent cation-suppressed conductance was observed in more than 90% of patches from rod cells and in several, but not all, patches from other retinal neurons in a total of 80 experiments in which the patch was excised into a bath solution lacking added  $\text{Ca}^{2+}$ .

The following experiments describe effects of  $\text{Mg}^{2+}$  rather than of  $\text{Ca}^{2+}$  because physiological levels of free  $\text{Mg}^{2+}$  (11) exceed those of free  $\text{Ca}^{2+}$  (12) in most cell types, and the divalent cation-suppressed conductance is thus more likely to be set by  $\text{Mg}^{2+}$  than by  $\text{Ca}^{2+}$  under physiological conditions. The dose-response relation of the divalent cation-suppressed conductance was examined under voltage-clamp conditions by applying a slow voltage ramp (50 mV/sec) to an inside-out, excised patch of rod outer segment membrane exposed to various bath concentrations of  $\text{Mg}^{2+}$  (Fig. 1B). Calcium and cGMP were not added to the bath solutions, and in order to avoid possible contamination with cGMP, this experiment was carried out with a superfusion apparatus that had never been exposed to cGMP and with culture dishes containing a low density of cells (<1 rod per square millimeter). The results obtained from experiments with 35 patches indicated that divalent cations suppressed an average of  $60.0 \pm 29.3$  pA at 50 mV and  $9.8 \pm 6.2$  pA at -50 mV (mean  $\pm$  SD). The free intracellular  $\text{Mg}^{2+}$  concentration estimated for non-rod cells is between 0.2 mM and 2 mM (11), well within the range of  $\text{Mg}^{2+}$  concentrations that affect the divalent cation-suppressed conductance.

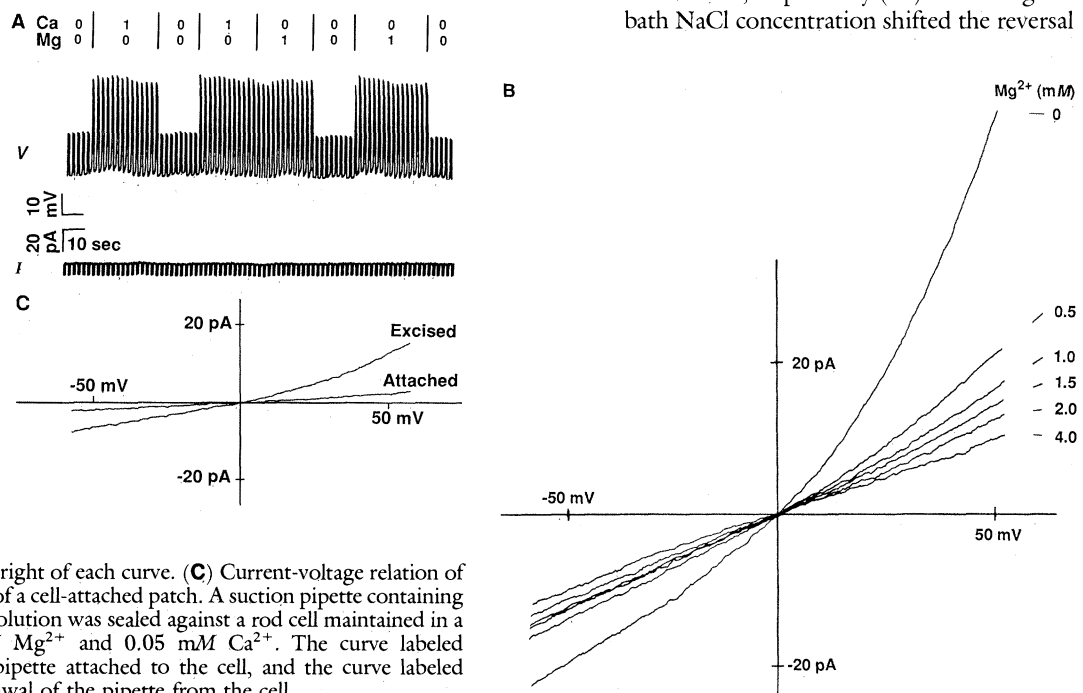
The current-voltage (*IV*) curves showed outward rectification in  $\text{Mg}^{2+}$  concentrations below 1 mM (Fig. 1B). The outward rectification in the absence of added divalent cations was similar in shape although less pronounced than that of the light-suppressed conductance of rod outer segments (13). When the curve obtained in the presence of 4 mM  $\text{Mg}^{2+}$  was subtracted from the others, however, the resulting family of *IV* curves showed rectification that resembled that of the light-suppressed (13) and cGMP-activated (1, 3, 4) conductances. The family of curves in Fig. 1B could not be made to overlap by simple scaling of the current. In addition, a nonscaling family of curves was obtained after subtracting the curve in the presence of 4 mM  $\text{Mg}^{2+}$  from the other curves. Such changes in the shape of the *IV* relation suggest that divalent cations do not simply alter the number of identical channels occupying a single open state. This is because each channel in a single open state would have the same microscopic *IV* curve, and simply summing identical microscopic curves would result in macroscopic curves with that same shape. Thus, although single-channel currents were not apparent at a resolution of 0.5 pA and 1 kHz, aspects of the macroscopic currents suggest that it is unlikely that the simplest two-state mechanism for channel regulation mediates the divalent cation-suppressed conductance.

Because the net conductance of the excised patch is the sum of the conductance of the excised membrane and of the seal between the pipette and membrane, we tested

for possible effects of divalent cations on the seal conductance at the pipette-membrane interface. This was done by measuring the conductance of cell-attached patches in which the seal was exposed to a bath solution containing a low concentration of divalent cations, while the intracellular face of the membrane was exposed to the cytoplasm. In about 90% of the cases, the conductance of the cell-attached patch was low when measured in bathing media containing 0.1 or 0.05 mM  $\text{Mg}^{2+}$  and  $\text{Ca}^{2+}$ . In about half of the cases, the conductance increased after excision and consequent exposure of the intracellular membrane face to the bath solution (Fig. 1C). Thus, although we cannot rule out the possibility that the seal conductance is, to some extent, modulated by divalent cations (14), it is unlikely that the seal is the major site of divalent cation action.

The permeability selectivity of the divalent cation-suppressed conductance for monovalent cations and anions was examined by measuring the conductance of an excised patch in the presence and absence of 2 mM  $\text{Mg}^{2+}$  in low or high NaCl concentrations (Fig. 2A). The upper pair of curves in Fig. 2A (Symmetric) show the *IV* relations of a patch exposed to the intracellular  $\text{Mg}^{2+}$  concentrations indicated to the right of each curve. These curves were obtained with standard monovalent ion concentrations, 120 mM  $\text{Na}^+$ , 3 mM  $\text{K}^+$ , and 123 mM  $\text{Cl}^-$ , in both the bath and the pipette. The lower pair of curves in Fig. 2A was recorded from the same patch at the same  $\text{Mg}^{2+}$  concentrations, but with the bath  $\text{Na}^+$  and  $\text{Cl}^-$  concentrations reduced to 34 and 37 mM, respectively (15). Reducing the bath NaCl concentration shifted the reversal

**Fig. 1.** (A) The effect of bath  $\text{Mg}^{2+}$  and  $\text{Ca}^{2+}$  on the conductance of an inside-out, excised patch of rod outer segment membrane. Under current-clamp conditions, 15-pA, 800-msec current pulses were applied to the membrane (current, *I*). The resulting voltage (*V*) deflections are inversely proportional to the patch conductance. The experiments were carried out with stock solutions. The pipette contained 2 mM  $\text{Mg}^{2+}$  and 2 mM  $\text{Ca}^{2+}$ . The bath contained the  $\text{Mg}^{2+}$  and  $\text{Ca}^{2+}$  concentrations indicated in millimolar units above the voltage record. (B) Current-voltage relation of the divalent cation-suppressed conductance under voltage-clamp conditions. The pipette solution contained 1 mM  $\text{Mg}^{2+}$  and 2 mM  $\text{Ca}^{2+}$ . The bath solution lacked added  $\text{Ca}^{2+}$  and contained the  $\text{Mg}^{2+}$  concentration indicated to the right of each curve. (C) Current-voltage relation of an excised patch compared with that of a cell-attached patch. A suction pipette containing 2 mM  $\text{Mg}^{2+}$  and 2 mM  $\text{Ca}^{2+}$  stock solution was sealed against a rod cell maintained in a bath solution containing 0.05 mM  $\text{Mg}^{2+}$  and 0.05 mM  $\text{Ca}^{2+}$ . The curve labeled "Attached" was recorded with the pipette attached to the cell, and the curve labeled "Excised" was recorded after withdrawal of the pipette from the cell.



potential of the divalent cation-suppressed conductance an average of  $+30.7 \pm 7$  mV ( $n = 15$  patches). This shift indicated that the divalent cation-suppressed conductance was much more permeable to monovalent cations than to anions because the reversal potential shifted toward the electrochemical equilibrium potential for  $\text{Na}^+$  (+33 mV) rather than toward that for  $\text{Cl}^-$  (-33 mV). The permeability selectivity of the cGMP-activated conductance was compared with that of the divalent cation-suppressed conductance by the same experimental protocol as in Fig. 2A (Fig. 2B). The reversal potential of the cGMP-activated conductance was shifted by  $+29.2 \pm 3.3$  mV ( $n = 5$  patches), as expected from a previous report (1) that indicated that the cGMP-activated conductance had cationic permeability selectiv-

ity. Thus, the divalent cation-suppressed and cGMP-activated conductances were nearly indistinguishable in terms of their relative permeabilities to cations and anions. Similar cation selectivity has also been observed for the light-suppressed conductance of the intact rod cell (12, 16).

The relative permeabilities of the patch membrane to  $\text{Na}^+$  and  $\text{K}^+$  were examined by exchanging  $\text{K}^+$  for  $\text{Na}^+$  in the bath solution. The lower pair of curves in Fig. 2C (Symmetric) shows the patch membrane conductance measured in the presence and absence of 2 mM  $\text{Mg}^{2+}$  with 120 mM  $\text{Na}^+$  and 3 mM  $\text{K}^+$  in both the bath and pipette. The upper pair of curves was taken from the same patch with the same  $\text{Mg}^{2+}$  concentrations, but with 3 mM  $\text{Na}^+$  and 120 mM  $\text{K}^+$  exposed to the intracellular side of the mem-

brane. The reversal potential for the divalent cation-suppressed conductance shifted an average of  $-10.6 \pm 1.6$  mV ( $n = 10$  patches) under conditions where the electrochemical equilibrium potential for sodium ( $E_{\text{Na}} = 96$  mV and  $E_{\text{K}} = -96$  mV, indicating that the divalent cation-suppressed conductance was slightly more permeable to  $\text{K}^+$  than to  $\text{Na}^+$ ). We then examined the relative permeabilities to  $\text{Na}^+$  and  $\text{K}^+$  of the cGMP-activated conductance (Fig. 2D). The lower pair of *IV* curves (Symmetric) was obtained with 120 mM  $\text{Na}^+$  and 3 mM  $\text{K}^+$  in both the bath and pipette, and the upper pair of curves was obtained with 3 mM  $\text{Na}^+$  and 120 mM  $\text{K}^+$  in the bathing medium. Exchanging the bath  $\text{Na}^+$  for  $\text{K}^+$  resulted in a shift of  $2.5 \pm 2.9$  mV ( $n = 5$  patches) in the reversal potential of the cGMP-activated conductance, indicating that, consistent with a previous report (1), the cGMP-activated conductance was slightly more permeable to  $\text{Na}^+$  than to  $\text{K}^+$ . Although there are clear similarities in terms of *IV* relations and roughly equal (although possibly not identical)  $\text{Na}^+ : \text{K}^+$  permeability ratios, it is not yet clear whether the conductances controlled by divalent cations and by cGMP arise from the same or different underlying molecule or molecules.

We further compared the divalent cation-suppressed and cGMP-activated conductances by measuring their sensitivities to the pharmacological agent *L-cis*-diltiazem. Current-voltage curves were measured from an inside-out patch under the following bathing conditions: (i) without added  $\text{Mg}^{2+}$ , (ii) in the presence of 20  $\mu\text{M}$  *L-cis*-diltiazem without added  $\text{Mg}^{2+}$ , and (iii) in the presence of 2 mM  $\text{Mg}^{2+}$  (Fig. 3A). *L-cis*-Diltiazem blocked more than 50% of the divalent cation-suppressed conductance in this experiment. On average, 25% of the divalent cation-suppressed conductance was blocked by 20  $\mu\text{M}$  *L-cis*-diltiazem in the 17 patches examined. Similar results were obtained in six experiments examining the effect of 30  $\mu\text{M}$  *L-cis*-diltiazem on the divalent cation-suppressed conductance. The effect of *L-cis*-diltiazem on the cGMP-activated conductance of the same patch illustrated in Fig. 3A is shown in Fig. 3B. The three curves were obtained in (i) the presence of 90  $\mu\text{M}$  cGMP, (ii) the absence of cGMP, and (iii) the presence of 20  $\mu\text{M}$  *L-cis*-diltiazem plus 90  $\mu\text{M}$  cGMP, with 1 mM  $\text{Mg}^{2+}$  present in each bath solution. Complete block of the cGMP-activated conductance, as expected from a previous report (4), was observed in a total of 48 patches. In some experiments, *L-cis*-diltiazem completely blocked the cGMP-activated conductance measured in the absence of divalent cations. The results in Fig. 3 further suggest that the divalent

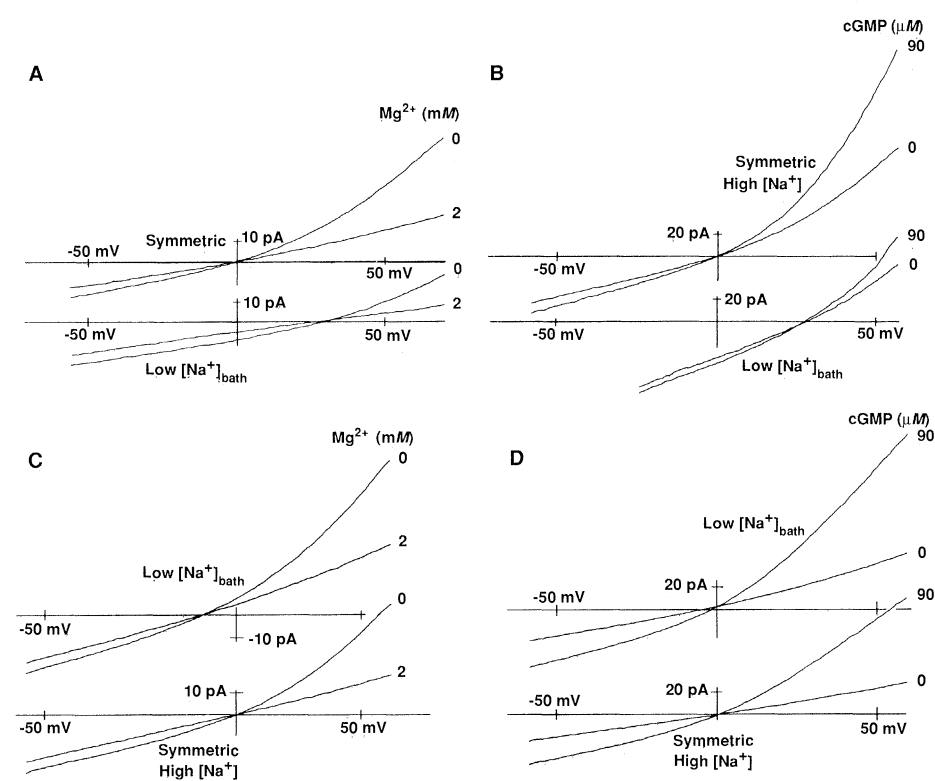
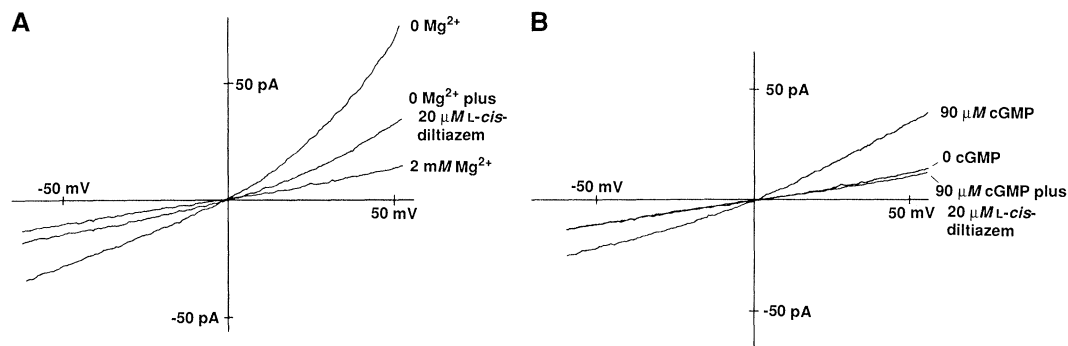


**Fig. 2.** (A) The monovalent cationic and monovalent anionic permeability of the divalent cation-suppressed conductance. The upper pair of *IV* curves (Symmetric) show the reversal potential of the divalent cation-suppressed conductance in the presence of the standard monovalent ion concentrations indicated below. The lower pair of *IV* curves (low $[\text{Na}^+]_{\text{bath}}$ ) show the reversal potential in the same patch, but after reducing the  $\text{Na}^+$  and  $\text{Cl}^-$  concentrations exposed to the intracellular side of the membrane to 34 mM and 37 mM, respectively. Experiments in all parts of this figure were with simple salt solutions with 2 mM  $\text{Mg}^{2+}$  and 2 mM  $\text{Ca}^{2+}$  in the pipette solution. Millimolar concentrations of  $\text{Na}^+$ ,  $\text{K}^+$ , and  $\text{Cl}^-$  were (bath/pipette) 120/120, 3/3, and 123/123, respectively, for symmetric curve pairs and 34/120, 3/3, and 37/123, respectively, for low $[\text{Na}^+]_{\text{bath}}$  curve pairs. (B) The monovalent cationic and monovalent anionic permeability of the cGMP-activated conductance. The upper pair of *IV* curves (Symmetric) show the reversal potential of the cGMP-activated conductance in the presence of symmetric monovalent ion concentrations. The same patch was used to obtain the lower pair of curves (low $[\text{Na}^+]_{\text{bath}}$ ) after lowering the bath  $\text{Na}^+$  to 34 mM and the bath  $\text{Cl}^-$  to 37 mM. The bath solution contained 1 mM  $\text{Mg}^{2+}$ . (C) The relative permeability of the divalent cation-suppressed conductance to  $\text{Na}^+$  and  $\text{K}^+$ . The lower pair of *IV* curves (Symmetric) were in the presence of standard ion concentrations. The upper pair of curves (low $[\text{Na}^+]_{\text{bath}}$ ) were from the same patch after reducing the bath  $\text{Na}^+$  concentration to 3 mM by replacing  $\text{Na}^+$  with  $\text{K}^+$ . (D) The relative permeability of the cGMP-activated conductance to  $\text{Na}^+$  and  $\text{K}^+$ . The bath solution contained 1 mM  $\text{Mg}^{2+}$ . The lower pair of *IV* curves (Symmetric) were in the absence or presence of 90  $\mu\text{M}$  cGMP in the bath with standard ion concentrations. The upper pair of *IV* curves (labeled low $[\text{Na}^+]_{\text{bath}}$ ) were from the same patch after reducing the bath  $\text{Na}^+$  concentration to 3 mM by replacing  $\text{Na}^+$  with  $\text{K}^+$ .

**Fig. 3. (A)** Resistance-of the divalent cation-suppressed conductance to blockade by *L-cis*-diltiazem. The *IV* curves in (A) and (B) were recorded from an inside-out, excised-patch of rod outer-segment membrane with simple salt solutions in both the bath and pipette, and with an additional 1 mM Mg<sup>2+</sup> and 2 mM Ca<sup>2+</sup> in the pipette. Exposure of the intracellular side of the patch to 2 mM Mg<sup>2+</sup> suppressed much of the outwardly rectifying conductance that was recorded in the absence of Mg<sup>2+</sup>.

Exposure of the patch to a bath solution lacking added Mg<sup>2+</sup> and containing 20 μM *L-cis*-diltiazem blocked only a component of the conductance, leaving a substantial component unblocked. **(B)** Blockade of the cGMP-activated



conductance by *L-cis*-diltiazem. These *IV* curves were obtained from the same patch as those in (A). Exposure of the intracellular side of the membrane to a bath solution containing 90 μM cGMP resulted in an outwardly rectifying con-

ductance. This conductance was blocked by 20 μM *L-cis*-diltiazem to levels below those recorded in the absence of cGMP. Each curve in (B) was recorded with 1 mM Mg<sup>2+</sup> in the bath solution.

cation-suppressed conductance did not arise from contaminant cGMP because concentrations of *L-cis*-diltiazem that were sufficient to block all of the cGMP-activated conductance blocked only part of the divalent cation-suppressed conductance. Interestingly, the light-suppressed conductance of the intact rod cell was also only partly blocked by 20 to 200 μM *L-cis*-diltiazem (4).

The presence of a conductance in excised patches of rod membrane that is sensitive to physiological concentrations of Mg<sup>2+</sup> led us to test the possibility that the cellular light response might also be sensitive to Mg<sup>2+</sup>. We recorded light responses from a voltage-clamped, dark-adapted rod cell in the presence of either 1 or 6 mM extracellular Mg<sup>2+</sup> (Fig. 4). The light responses were recorded under voltage-clamp conditions by means of the intracellular dialysis or whole-cell patch-clamp technique with an intracellular solution containing 90 mM potassium aspartate, 20 mM sucrose, 10 mM NaH<sub>2</sub>PO<sub>4</sub>, 4 mM MgCl<sub>2</sub>, 1 mM disodium salt of adenosine 5'-triphosphate, and 0.05 mM EGTA titrated to pH 7.3 with KOH (4). The holding potential was approximately 10 mV more hyperpolarized than the dark-adapted resting potential. The left record of Fig. 4 shows

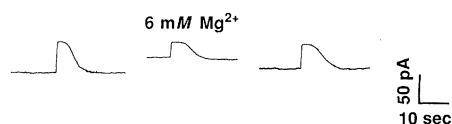


**Fig. 4.** The effect of Mg<sup>2+</sup> on the light response of an intact rod cell. The current records were obtained from a dark-adapted rod cell with the intracellular dialysis (or whole-cell patch-clamp) technique. Suprasaturating light flashes were used. The record on the left was obtained in the presence of 1 mM extracellular Mg<sup>2+</sup>. Changing the superfusion solution to one containing 6 mM Mg<sup>2+</sup> resulted in a decrease in the holding current and an approximately equal decrease in the light response amplitude (middle trace). The light response in the right record was after returning to the original superfusion solution containing 1 mM Mg<sup>2+</sup>.

the response to a saturating light flash obtained in the presence of 1 mM Mg<sup>2+</sup>. The baseline current of approximately -70 pA recorded in the dark was transiently suppressed by a saturating light flash. The middle record was obtained immediately after exposing the cell to 6 mM Mg<sup>2+</sup>. Elevated Mg<sup>2+</sup> decreased the baseline current and light response amplitudes by approximately equal amounts (35 pA) and increased the plateau light-response duration by about 2.5 seconds. Previously reported voltage recording from rods in the intact toad retina did not reveal an effect of Mg<sup>2+</sup> (17), possibly because of countereffects on voltage-dependent conductances. The effects of Mg<sup>2+</sup> were, in large part, reversible (Fig. 4, right trace). The results in Fig. 4 show that the phototransduction mechanism contains a divalent cation-sensitive site, perhaps the cGMP-activated conductance (3), the divalent cation-suppressed conductance, or an as yet unidentified site. Although the result is consistent with the presence of the divalent cation-suppressed conductance in the intact cell, it does not directly demonstrate the conductance.

The results in Fig. 1 show that divalent cations directly suppressed a conductance in excised patches of rod cell membrane in the absence of cGMP. The divalent cation-suppressed conductance was sensitive to concentrations of Mg<sup>2+</sup> over the standard physiological range. The divalent cation-suppressed conductance was large considering the small area of the patch membrane. The current density induced by changing from 0.5 mM Mg<sup>2+</sup> to no added Mg<sup>2+</sup> was approximately 5 pA/μm<sup>2</sup> in the range of membrane potential from -30 to -60 mV, which is large compared to the 0.05 pA/μm<sup>2</sup> of light-suppressed current density recorded from the rod cell (8, 18). Thus, the divalent cation-suppressed conductance, like the cGMP-activated conductance, was more than 100 times larger than the conductance

that underlies the cellular light response. This raises the possibility that changes in intracellular free Mg<sup>2+</sup> could be significant in the control of visual transduction.

Although we have focused on the effects of Mg<sup>2+</sup>, both Ca<sup>2+</sup> and Mg<sup>2+</sup> can affect the conductance of excised patches. Light-dependent control of the membrane conductance by either divalent cation will depend, in large part, on the background activities of divalent cations as well as of cGMP and on the polarity of the activity change. In the case of Ca<sup>2+</sup>, one of the original candidates for the intracellular messenger mediating the light response (18), there are indications that the activity of Ca<sup>2+</sup> decreases during the light response (12, 13, 19), which, by the mechanism described here, would lead to a conductance increase. In the case of Mg<sup>2+</sup>, although steady light is known to affect the total Mg<sup>2+</sup> content of the rod outer segment (20), little is known about the effect of light on free intracellular Mg<sup>2+</sup>. The observation that the rod membrane conductance is sensitive to a number of agents suggests that several factors should be considered in a quantitative description of the light-regulated conductance change in the outer segment. Our present picture of phototransduction is one of dual control of the rod outer-segment conductance by cGMP and by divalent cations. Parallel intracellular pathways might provide the cell with an increased flexibility for responding to a wide range of light conditions.

#### REFERENCES AND NOTES

1. E. E. Fesenko *et al.*, *Nature (London)* **313**, 310 (1985).
2. A. L. Zimmerman *et al.*, *Proc. Natl. Acad. Sci. U.S.A.* **82**, 8813 (1985).
3. G. Matthews, *J. Neurosci.* **6**, 2521 (1986).
4. J. H. Stern, U. B. Kaupp, P. R. MacLeish, *Proc. Natl. Acad. Sci. U.S.A.* **83**, 1163 (1986).
5. L. W. Haynes, A. R. Kay, K.-W. Yau, *Nature (London)* **321**, 66 (1986); A. L. Zimmerman and D. A. Baylor, *ibid.*, p. 70.
6. O. P. Hamill *et al.*, *Pfluegers Arch.* **391**, 85 (1981).
7. The intracellular side of the membrane is exposed to

- the bath during experiments using inside-out, excised patches. In this convention, the membrane potential is given as the voltage at the intracellular side of the membrane minus the voltage at the extracellular side of the membrane.
8. C. R. Bader *et al.*, *J. Physiol. (London)* **296**, 1 (1979).
  9. In solutions lacking added divalent cations, roughly 10 to 20  $\mu\text{M}$  divalent cations are expected because of contamination from the distilled water, NaCl, and other sources.
  10. Because conductance was measured under current-clamp conditions, the conductance decrease shown is a lower limit.
  11. Estimates of intracellular free  $\text{Mg}^{2+}$  concentration range from approximately 0.2 mM to 2 mM [D. Maughan and C. Recchia, *J. Physiol. (London)* **368**, 545 (1985)]. The range of estimates of free  $\text{Mg}^{2+}$  is well above the submicromolar levels of intracellular free  $\text{Ca}^{2+}$  estimated to be present in rod cells (12).
  12. P. A. McNaughton, L. Cervetto, B. J. Nunn, *Nature (London)* **322**, 261 (1986).
  13. P. R. MacLeish, E. A. Schwartz, M. Tachibana, *J. Physiol. (London)* **348**, 645 (1984).
  14. Experiments were carried out in the presence of 0.1 or 0.05 mM  $\text{Mg}^{2+}$  and  $\text{Ca}^{2+}$  because rapid deterioration of cells was observed in the absence of added divalent cations. We assume that the lack of divalent cation-suppressed conductance in half of these patches was due to the formation of sealed vesicles, which is known to occur in the presence of bath  $\text{Ca}^{2+}$  (6). Other evidence suggesting that the divalent cation-suppressed conductance resides in the membrane rather than the seal is that the size of the divalent cation-suppressed conductance was not obviously correlated with the net conductance of the patch (that is, seal plus membrane). Furthermore, R. Coronado [*Biophys. J.* **47**, 851 (1986)] reported that, although pure lipid membranes composed primarily of negatively charged lipid did result in a divalent cation-dependent seal conductance, seals formed with pure lipids with a composition similar to that of the rod outer segment [E. H. Drenth *et al.*, *Biochim. Biophys. Acta* **603**, 130 (1980); G. P. Miljanich, P. P. Nemes, D. L. White, E. A. Dratz, *J. Membr. Biol.* **60**, 249 (1981)] were largely independent of divalent cations.
  15. Zero current and voltage were defined as the crossing point of the curves in symmetric conditions of monovalent ions. Results similar to those of Fig. 2, A and B, were obtained when NaCl was replaced by iso-osmotic amounts of sucrose, indicating that the observed changes in conductance did not arise from changes in osmotic strength. The combination of junction and streaming potentials measured with a 3M KCl electrode for the various solutions in Fig. 2, C and D, were less than, and usually much less than, 4 mV.
  16. M. L. Woodruff, B. L. Bastain, G. L. Fain, *J. Gen. Physiol.* **80**, 517 (1982); M. Capovilla *et al.*, *J. Physiol. (London)* **343**, 295 (1983); K.-W. Yau and K. Nakatani, *Nature (London)* **309**, 352 (1984).
  17. J. E. Brown and L. H. Pinto, *J. Physiol. (London)* **236**, 575 (1974).
  18. W. A. Hagins, *Annu. Rev. Biophys. Bioeng.* **1**, 131 (1972); ——— and S. Yoshikami, *Exp. Eye Res.* **18**, 299 (1974).
  19. G. H. Gold and J. I. Korenbrot, *Proc. Natl. Acad. Sci. U.S.A.* **77**, 5557 (1980); S. Yoshikami *et al.*, *Nature (London)* **286**, 395 (1980); K.-W. Yau and K. Nakatani, *ibid.* **313**, 579 (1985); H. R. Matthews *et al.*, *ibid.*, p. 582; G. H. Gold, *Proc. Natl. Acad. Sci. U.S.A.* **83**, 1150 (1986).
  20. A. P. Somlyo and B. Walz, *J. Physiol. (London)* **358**, 183 (1985).
  21. We thank T. Wiesel for continued support, suggestions, and encouragement, and J. Lisman and S. Temple for their comments on a previous version of this manuscript. The basic observations described here have been reported in an earlier abstract [J. H. Stern, H. Knutsson, P. R. MacLeish, *Invest. Ophthalmol. Visual Sci.* **27**, 301a (1986)]. Funding for this work was from NIH grant EY05201, NIH fellowship EY05730, the Klingenstein Fund, the Alfred P. Sloan Foundation, and a Senator Jacob Javits Center for Excellence in Neuroscience Award (NS-22789).

9 September 1986; accepted 17 April 1987

## The Visual Cycle Operates via an Isomerase Acting on All-*trans* Retinol in the Pigment Epithelium

C. DAVID BRIDGES AND RICHARD A. ALVAREZ

Thirty years have elapsed since Wald and his colleagues showed that 11-*cis* retinal was isomerized to all-*trans* when rhodopsin was bleached, yet little has been understood about the reverse process that generates 11-*cis* retinal for rhodopsin regeneration. It is not known whether the isomerization is enzyme-mediated, whether it occurs in the pigment epithelium or in the retina, or whether retinal, retinol, or a retinyl ester is the vitamin A compound that is isomerized. Radiolabeled all-*trans* retinol and high-performance liquid chromatography have now been used to demonstrate the existence of an eye-specific, membrane-bound enzyme (retinol isomerase) that converts all-*trans* to 11-*cis* retinol in the dark. Retinol isomerase is concentrated in the pigment epithelium; this localization clarifies the role of this tissue in rhodopsin regeneration and explains the need to transfer all-*trans* retinol from the rod outer segments to the pigment epithelium during the visual cycle.

THE ISOMERIZATION OF ALL-*trans* retinoids to the 11-*cis* configuration is essential for visual pigment regeneration in the eye (1). A "retinal isomerase" originally reported by Hubbard (2) apparently acted by photoisomerization of an artifactually generated protonated Schiff base composed of all-*trans* retinal and phosphatidylethanolamine (3). Furthermore, this observation is probably not physiologically significant, because exposure to potentially

isomerizing light does not influence the course of dark adaptation in vertebrates (4). Although it had been suggested that the isomerization may not be enzyme-mediated, recent data by the same authors that appeared since the present work was submitted demonstrate a retinol-specific isomerase in pigment epithelium (5). Here we have studied frogs and rats because the visual cycle has been extensively investigated in these animals (6, 7). We present evidence that both

species possess an eye-specific, membrane-bound enzyme that converts all-*trans* to 11-*cis* retinol in the dark and therefore fulfills the primary requirement for an isomerase that plays a central role in dark adaptation. Although earlier evidence suggested otherwise (6, 8, 9), this isomerase is concentrated in the pigment epithelium.

We centrifuged homogenates of combined retina, pigment epithelium, and choroid from light- or dark-adapted frogs at 700g to pellet the nuclei and unbroken cells, then incubated the supernatants in darkness with all-*trans* [ $^3\text{H}$ ]retinol. After 3 hours, we extracted the mixture and found that the major radiolabeled vitamin A compound (excluding all-*trans* retinol) was 11-*cis* retinol (Table 1). The very low levels of radioactivity associated with 11-*cis* retinyl palmitate confirm *in vitro* studies (9) and are also consistent with the very slow appearance of labeled 11-*cis* retinyl palmitate in the eyes of living frogs injected with all-*trans* [ $^3\text{H}$ ]retinol (9). The higher proportion of retinyl ester formed by the 700g pellet indicates that there was some enrichment of the ester synthase in this fraction. Our subsequent experiments focused on the formation of 11-*cis* retinol by the 700g supernatant with protein concentrations of 0.3 to 11.8 mg/ml.

A typical set of data is shown in Fig. 1. The high-performance liquid chromatography (HPLC) tracing from the absorbance detector (Fig. 1, top) shows that the endogenous retinol isomers extracted from the incubation mixture are mainly 11-*cis* (0.52 nmol) and all-*trans* (0.24 nmol), with a small amount of 13-*cis* (0.03 nmol) but no detectable 9-*cis* (in other experiments, traces of the 9-*cis* isomer were variably present). The radioactivity profile (Fig. 1, center) shows a prominent peak (25% of the total extracted radiolabeled retinol isomers) that coelutes with 11-*cis* retinol and a smaller peak (8% of the total radiolabel) that coelutes with 13-*cis* retinol. The truncated peak (59% of the radioactivity) coelutes with the all-*trans* retinol substrate (Fig. 1, bottom). We did not identify the remaining peaks, but observed them consistently in most experiments.

To confirm the identities of the labeled presumptive 11-*cis* and 13-*cis* retinols, they were collected from the column, oxidized to the aldehydes with activated manganese dioxide (10, 11), and mixed with unlabeled authentic 11-*cis*, 13-*cis*, and all-*trans* retinal. Analysis by HPLC (10) showed that the oxidation procedure had yielded the corresponding labeled 11-*cis* and 13-*cis* retinal

Department of Ophthalmology, Baylor College of Medicine, Houston, TX 77030.